

International Journal of Computational Methods
© World Scientific Publishing Company

FIXED GRID FINITE ELEMENT ANALYSIS FOR 3D STRUCTURAL PROBLEMS*

MANUEL J. GARCÍA, MIGUEL A. HENAO and OSCAR E. RUIZ

*Department of Mechanical Engineering, EAFIT University,
Cr 47 No. 7 sur 50 Medellin, Antioquia, Colombia,
mgarcia@eafit.edu.co*

Received (Day Month Year)

Revised (Day Month Year)

Fixed Grid (FG) methodology was first introduced by García and Steven as an engine for numerical estimation of two-dimensional elasticity problems. The advantages of using FG are simplicity and speed at a permissible level of accuracy. Two dimensional FG has been proved effective in approximating the strain and stress field with low requirements of time and computational resources. Moreover, FG has been used as the analytical kernel for different structural optimisation methods as Evolutionary Structural Optimisation, Genetic Algorithms (GA), and Evolutionary Strategies. FG consists of dividing the bounding box of the topology of an object into a set of equally sized cubic elements. Elements are assessed to be inside (I), outside (O) or neither inside nor outside (NIO) of the object. Different material properties assigned to the inside and outside medium transform the problem into a multi-material elasticity problem. As a result of the subdivision NIO elements have non-continuous properties. They can be approximated in different ways which range from simple setting of NIO elements as O to complex non-continuous domain integration. If homogeneously averaged material properties are used to approximate the NIO element, the element stiffness matrix can be computed as a factor of a standard stiffness matrix thus reducing the computational cost of creating the global stiffness matrix. An additional advantage of FG is found when accomplishing re-analysis, since there is no need to recompute the whole stiffness matrix when the geometry changes.

This article presents CAD to FG conversion and the stiffness matrix computation based on non-continuous elements. In addition inclusion/exclusion of O elements in the global stiffness matrix is studied. Preliminary results shown that non-continuous NIO elements improve the accuracy of the results with considerable savings in time. Numerical examples are presented to illustrate the possibilities of the method.

Keywords: Fixed Grid Finite Element Analysis; Interactive Design.

1. Introduction

Fixed Grid (FG) as a methodology to solve elasticity problems was first introduced by García and Steven, (1998, 1999a, 1999b) as an engine for numerical estimation of

*Preliminary results of this investigation were presented at the Sixth World Congress on Computational Mechanics (WCCM VI) Beijing, China.

stress and displacement fields. The advantages of using FG are simplicity and speed at a permissible level of accuracy. In FG the stress error was seen to increase near the region of stress concentration, with a maximum stress error being approximately 10% for a reasonably-sized mesh. However, the average stress error was found to be about 5% or below and the displacement field error was even lower, around 1% [García and Steven (1996)]. Thus, the FG method was deemed as appropriate for interactive design and structural optimisation where highly accurate analysis is not needed.

A Fixed Grid is generated by superimposing a rectangular grid of equal-sized elements on the given structure instead of generating a mesh to fit to the structure. In this way, elements are either inside (*I*), outside (*O*), or on the boundary (*NIO*) of the structure. An *O* element is given a material property of a non-interactive media. That is, its value is significantly less than the property of an *I* element. This transforms the problem into a bi-material one. *NIO* elements are constituted by two types of material and therefore their properties are not continuous over the element. Different methods can be used to approximate *NIO* elements. That includes from dropping them as *O* elements to complex non-continuous domain integration. If averaged material properties are used to approximate the *NIO* element properties, then the element-stiffness matrix can be computed as a factor of a standard stiffness matrix. therefore the assembly of the system matrix can be accomplished efficiently. An additional advantage is found when the shape of the structure is changed in response to a previous analysis. The global structure of the FG is maintained, and re-computation of the new stiffness matrix can be accomplished by changing only the positions affected by the elements whose *I*, *O*, and *NIO* state has changed [García and Steven (2000)].

The application of FG-FEA to two-dimensional linear elastic problems has been a research topic during the last years, see [García (1999a)]. It has been proved effective in approximating the strain and stress field with low requirements of time and computational resources. Moreover, FG-FEA was used as the mathematical kernel for different structural optimisation methods like: Evolutionary Structural Optimisation (ESO) [Kim *et al.* (2000)], Genetic Algorithms (GA) [Woon *et al.* (2000)], and Evolutionary Strategies (ES) [García and Gonzalez (2004)].

Previous work has been done with three-dimensional linear elastic structures by Suzuki and Ohtsubo [Suzuki *et al.* (1998)]. Boundary conditions are applied by further subdividing the boundary elements (multi-scale voxel) thus requiring a less general resolution. The present approach presents some improvements to the local stiffness matrix and force vector calculations for *NIO* elements by considering them as non-continuous elements. Also the inclusion or exclusion of *O* elements in the global stiffness matrix is studied. Finally, preliminary results of this investigation were presented at the Sixth World Congress on Computational Mechanics [Garcia *et al.* (2004)]

1.1. Definitions

Let Ω_{FG} denote the smallest bounding box that completely encloses the domain Ω and is oriented along the axes of the coordinate system, that is

$$\Omega_{FG} = \left\{ \mathbf{x} \mid \min_{\mathbf{y} \in \Omega} (y_i) \leq x_i \leq \max_{\mathbf{y} \in \Omega} (y_i) \right\}, \quad (1)$$

then Ω_{FG} is called the **fixed grid domain** in this study. A point $\mathbf{x} \in \Omega_{FG}$ is considered *inside* if $\mathbf{x} \in \Omega$. A point $\mathbf{x} \in \Omega_{FG}$ is considered *outside* if $\mathbf{x} \notin \Omega$. In order to preserve characteristics of the original problem, the material properties of an outside point are the properties of a non-interactive medium. The object is embedded into a box made of non interactive material. Notice that this definition transforms the elastic problem into a bi-material problem. Figure 1 shows examples of a fixed grid domain for two-dimensional and three-dimensional cases. The domain is completely defined by the points \mathbf{x}_{min} and \mathbf{x}_{max} that define the maximum and minimum points that belong to Ω_{FG} .

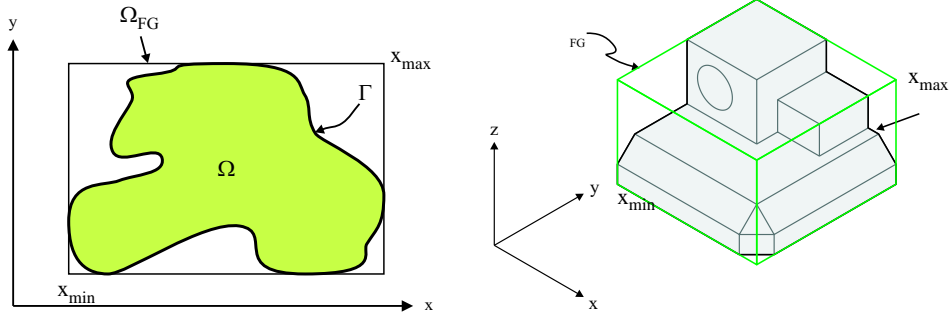


Fig. 1. Typical two- and three-dimensional fixed grid domains

In order to obtain the FG, the fixed grid domain, Ω_{FG} , is subdivided into a set of cubic elements with dimensions h_1, h_2, h_3 . See Figure 2.

An **element** is each one of the cells, of dimension $h_1 \times h_2 \times h_3$, in which Ω_{FG} is subdivided. The elements $e_m, m = 0, \dots, n_e - 1$ are numbered in ascending order from the one containing the minimum point \mathbf{x}_{min} in the direction of the x axis, then in the y axis, and finally in the z axis. An element e_m can be associated by its index in each dimension $e_m = e_{ijk}$, that is, row, column, and floor of the element in the grid. The element domain Ωe_m is defined as $\Omega e_m = \{ \mathbf{x} \mid \mathbf{x} \in e_m \}$, and its boundary is denoted as $\partial \Omega e_m$.

The **nodes** are the vertices of the elements in the FG. Each element $e_m = e_{ijk}$ has eight nodes n_j , with $j = 0..7$. A node in the FG is classified as an **inside node** if $n_j \in \Omega$ and as an **outside node** if $n_j \notin \Omega$.

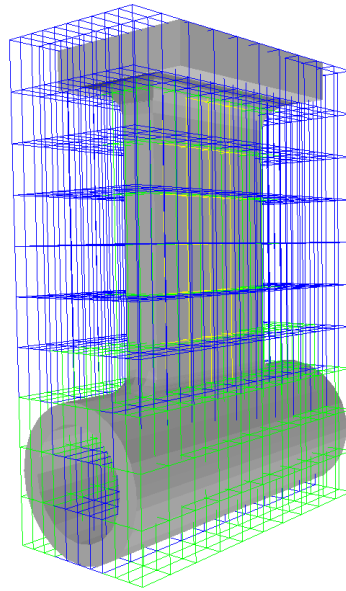


Fig. 2. Three-dimensional Fixed Grid

1.2. *Element Classification*

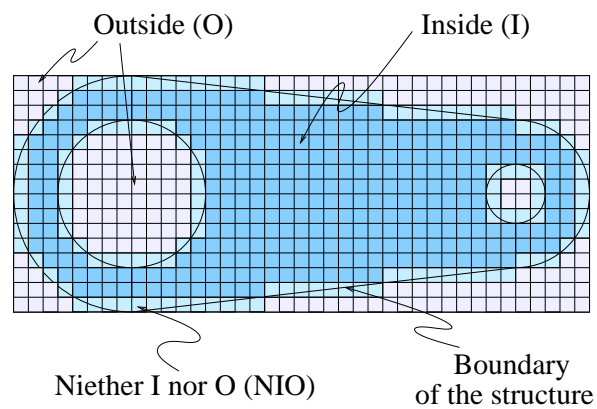


Fig. 3. Fixed grid approximation of the geometry of a structure showing the different types of finite elements

According to the position of the elements with respect to the structure, they

can be classified as three different types: an element e_m is called I (*Inside*) if for all $\mathbf{x} \in e_m, \mathbf{x} \in \Omega$. An element is called O (*Outside*) if for all $\mathbf{x} \in e_m, \mathbf{x} \notin \Omega$, that is, the element consists of only points external to Ω . An element is called NIO (*Neither Inside nor Outside*) if there exist points $\mathbf{x}, \mathbf{y} \in e_m$ such that $\mathbf{x} \in \Omega$ and $\mathbf{y} \notin \Omega$. That means, the element has points inside as well as outside of Ω (these are elements on the boundary of the structure). Figure 3 illustrates the different types of elements for a given structure. These elements differ only in their material properties. Elements I have the material properties of the structure, elements O the material properties of a non-active medium, and elements NIO have both material properties.

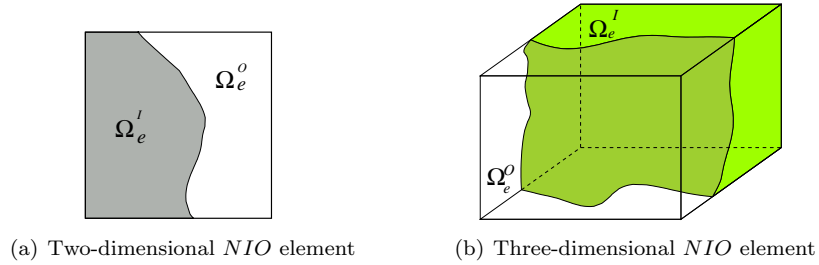


Fig. 4. NIO Element. An element with discontinuous material properties

This representation of the domain facilitates the process of analysis as it does not require sophisticated and high order algorithms to generate the mesh. Furthermore, it will be shown that the local stiffness matrix is the same for all the elements and it only needs to be computed once for the whole analysis

An elements e_m can be classified according to its nodes types as

$$\text{type}(e_m) = \begin{cases} I & \text{if } n_j \in e_i \Rightarrow n_j \in \Omega \\ O & \text{if } n_j \in e_i \Rightarrow n_j \notin \Omega \\ NIO & \text{Otherwise} \end{cases} . \quad (2)$$

This criteria is not exact as there are cases where the element is classified as I or O when it actually is NIO . These cases are presented when the B-Rep of the object intersects the element at the face of the cube without touching any of the vertices, for example, a cone end or a pyramid vertex penetrating the face of an element. These cases are the result of small details in the geometry of the object which are not captured by the fixed grid resolution. The important point to notice here is that it may or not be desirable to capture the detail of the geometry for analysis purposes. In general, CAD data needs to be *defeatured* by removing excessive detail that only adds noise to the analysis. This is of particular interest at the initial stages of the design [Mobley *et al.* (1998)].

2. General description of Fixed Grid generation

A Finite Element preprocessor takes the geometry of a structure usually represented by its boundary representation (B-Rep) and subdivides it into a set of finite elements of different shapes and sizes. A fixed grid preprocessor is a specialised version of a finite element preprocessor where all the elements have fixed geometry but different physical properties. Furthermore, the boundary conditions must be properly codified into this new representation. The fixed grid preprocessing or conversion of the B-Rep geometry into a fixed grid representation is accomplished in the following steps: (i) Fixed Grid domain computation, (ii) node classification, (iii) B-Rep subdivision to suit the element size, (iv) element classification (I , O , NIO), (v) computation of NIO geometry and volume, and (vi) boundary condition assignment.

3. Fixed Grid Finite Element Analysis

The discrete form of finite element formulation for linear elastic material can be stated as

$$[K] \{u_S\} - \{F\} = 0 \quad (3)$$

where $[K]$ is the stiffness matrix of the system, u_S is the vector of displacements, and F represents the vector of forces. Additionally, the stiffness matrix $[K]$ can be constructed from element stiffness matrices $[K^{(e)}]$ as,

$$[K] = \sum_{e=1}^E [K^{(e)}] = \sum_{e=1}^E \int_{\Omega^{(e)}} [B]^T [C] [B] d\Omega, \quad (4)$$

where $[B]$ is a matrix containing derivatives of the shape functions and $[C]$ is the tensor of material properties. For isotropic materials $[C]$ is given by

$$[C] = \frac{E}{(1+\nu)(1-2\nu)} \begin{bmatrix} 1-\nu & \nu & \nu & 0 & 0 & 0 \\ \nu & 1-\nu & \nu & 0 & 0 & 0 \\ \nu & \nu & 1-\nu & 0 & 0 & 0 \\ 0 & 0 & 0 & \frac{1}{2}-\nu & 0 & 0 \\ 0 & 0 & 0 & 0 & \frac{1}{2}-\nu & 0 \\ 0 & 0 & 0 & 0 & 0 & \frac{1}{2}-\nu \end{bmatrix} \quad (5)$$

with E the Young modulus and ν the Poisson's ratio.

Computation of integrals in (4) depends upon the shape and material of the element. Due to its complexity the integrals are usually calculated by using isoparametric elements and numerical integration [Fagan, M.J. (1992)].

3.1. The Fixed Grid method

In traditional FEA the domain is subdivided into a set of elements that fit its shape. The most common algorithm to subdivide the domain is known as Delone triangulation. The result of such algorithms is a set of irregularly shaped elements. Construction of stiffness matrix $[K]$ implies computation of the integral defined in (4) for each element in the mesh. In contrast, all the elements of a FG have the same shape but different material properties. However, as it was shown in the previous section there are only three types of elements: I , O , and NIO . The following section develops the computation of the stiffness matrix for the homogeneous I and O elements and then for the non-homogeneous NIO elements.

3.2. Stiffness matrix for I and O elements

From (5) it can be observed that $[C]$ depends only on the Young modulus and the Poisson's ratio. Then, it is possible to express $[C]$ as the sum of two matrices $[F']$ and $[G']$ in the following way,

$$[C] = k (\nu [F'] + [G']) \quad (6)$$

where $k = \frac{E}{(1 + \nu)(1 - 2\nu)}$, and

$$[F'] = \nu \begin{bmatrix} -1 & 1 & 1 & 0 & 0 & 0 \\ 1 & -1 & 1 & 0 & 0 & 0 \\ 1 & 1 & -1 & 0 & 0 & 0 \\ 0 & 0 & 0 & -1 & 0 & 0 \\ 0 & 0 & 0 & 0 & -1 & 0 \\ 0 & 0 & 0 & 0 & 0 & -1 \end{bmatrix}, \quad [G'] = \begin{bmatrix} 1 & 0 & 0 & 0 & 0 & 0 \\ 0 & 1 & 0 & 0 & 0 & 0 \\ 0 & 0 & 1 & 0 & 0 & 0 \\ 0 & 0 & 0 & \frac{1}{2} & 0 & 0 \\ 0 & 0 & 0 & 0 & \frac{1}{2} & 0 \\ 0 & 0 & 0 & 0 & 0 & \frac{1}{2} \end{bmatrix}. \quad (7)$$

Because of (6) it is possible to redefine (4) as

$$\begin{aligned} [K^{(e)}] &= \int_{\Omega^{(e)}} [B]^T [k (\nu [F'] + [G'])] [B] d\Omega \\ &= k \left\{ \nu \int_{\Omega^{(e)}} [B]^T [F'] [B] d\Omega + \int_{\Omega^{(e)}} [B]^T [G'] [B] d\Omega \right\} \\ &= k \left\{ \nu \int_{\Omega^{(e)}} [F] d\Omega + \int_{\Omega^{(e)}} [G] d\Omega \right\} \end{aligned} \quad (8)$$

where $[F] = [B]^T [F'] [B]$ and $[G] = [B]^T [G'] [B]$. Additionally ν is taken out of the integral because it is constant over $\Omega^{(e)}$.

The computation of $[K^{(e)}]$ by (8) allows the separation between the mechanical properties of the material and the geometry of the element. Given that all the elements in the FG have the same geometry then the integrals over $[F]$ and $[G]$ are the same and need only to be computed once.

3.3. Stiffness matrix for *NIO* elements

A typical *NIO* element is shown in Figure 4. These elements intersect the boundary of the structure so they are subdivided between two parts $\Omega_e = \Omega_e^I \cup \Omega_e^O$. Here $\Omega_e^I = \Omega \cap \Omega_e$ represents the part of the element with *I* material properties and $\Omega_e^O = \Omega_e - (\Omega \cap \Omega_e)$ the part of the element with *O* material properties. This discontinuity in $[C]$ represent a complexity in the computation of $[K_e]$. However, computation of $[K_e]$ can be approximated in different ways. Two possible approximations are presented next.

3.3.1. Discrete approximation—A0

This is the simplest way of computing the integrals and consists of approximating the *NIO*'s elements as *I* or *O* depending on the amount of element inside the structure. Because the material properties are allowed to take only discrete values (*I* or *O* material properties) this approximation is referred to as discrete approximation.

If $V = \text{volume}(\Omega_e)$, and $V_I = \text{volume}(\Omega_e^I)$ then, according to the A0 approximation, the material properties E and ν of an *NIO* element are given by

$$(E_{NIO}, \nu_{NIO}) = \begin{cases} (E_I, \nu_I) & \text{if } V_I/V > 1/2 \\ (E_O, \nu_O) & \text{if } V_I/V \leq 1/2 \end{cases} . \quad (9)$$

Numerical experiments in the two-dimensional case have shown that AO approximation presents a large error in the displacement and stress fields. To reduce the error it is necessary to decrease the size of the elements in the grid. As a consequence of this mesh refinement there will be an increasing computational cost of the analysis [García (1999a); García and Steven (1997)].

3.3.2. Weighted average approximation—A1

This is a more precise, but still an approximate method to represent the elements on the boundary. *NIO* elements are constituted by two different materials (*I* and *O* materials). A1 approximation transforms the bi-material element into a homogeneously isotropic element with material properties that best simulate the non-continuous element. Thus a property will be the weighted average of the *I* and *O* properties:

$$\begin{aligned} \nu_{NIO} &= \nu_I \xi + \nu_O (1 - \xi) \\ E_{NIO} &= E_I \xi + E_O (1 - \xi) \end{aligned} \quad (10)$$

where ξ is equal to the ratio $\xi = V_I/V$.

Finally, A0 and A1 approximate an *NIO* element as homogeneous by applying (9) and (10). Therefore, (8) can be used in both cases to compute the element stiffness matrix.

4. Point Forces

Punctual forces applied over a boundary should be translates into adequate nodes of *NIO* or boundary elements.

Let H be a hexahedral finite element with eight nodes. The shape functions for the element H can be obtained from the equation:

$$\omega(x, y, z) = \alpha_1 + \alpha_2x + \alpha_3y + \alpha_4z + \alpha_5xy + \alpha_6yz + \alpha_7zx + \alpha_8xyz. \quad (11)$$

The resulting shape functions [Zienkiewicz and Taylor (1994)] for the nodes of an element H with node one at position (x_0, y_0, z_0) [see figure 5(a)] can be expressed as a vector \mathbf{N} of size 8 as

$$\mathbf{N} = \frac{1}{hx \ hy \ hz} \begin{bmatrix} -(z_0 + hz - z)(y_0 + hy - y)(x - x_0 - hx) \\ (z_0 + hz - z)(y_0 + hy - y)(x - x_0) \\ -(z_0 + hz - z)(y_0 - y)(x - x_0) \\ (z_0 + hz - z)(y_0 - y)(x - x_0 - hx) \\ (z_0 - z)(y_0 + hy - y)(x - x_0 - hx) \\ -(z_0 - z)(y_0 + hy - y)(x - x_0) \\ (z_0 - z)(y_0 - y)(x - x_0) \\ -(z_0 - z)(y_0 - y)(x - x_0 - hx) \end{bmatrix}. \quad (12)$$

Every component of \mathbf{N} represents the shape function for the node i with $i = 1, \dots, 8$. By the properties of \mathbf{N} , for any $\mathbf{x} \in \mathbb{R}^3$ the sum of the shape functions is equal to one, $\sum_{i=1}^8 N_i(\mathbf{x}) = 1$. Furthermore, if $\mathbf{x} \in H$ then $0 \leq N_i(\mathbf{x}) \leq 1$. Then the domain represented by H can be defined as:

$$H = \left\{ \mathbf{x} \mid \sum_{i=1}^8 N_i(\mathbf{x}) = 1, \wedge, N_i(\mathbf{x}) \in [0, 1], i = 1, \dots, 8 \right\}. \quad (13)$$

This property can be used to relocate a force \mathbf{F} applied at a point inside an *NIO* element. If a force \mathbf{F} is applied at a point \mathbf{x} inside the domain of H and \mathbf{x} [figure 6(a)] is not located at the nodes of the element, then \mathbf{F} can be replaced by a set of forces \mathbf{G}_i distributed over all the nodes of H [see figure 6(b)].

Then the resulting set of forces applied to the element nodes can be computed as a weighted set using the element shape functions N_i . That is:

$$\mathbf{F} = \sum_{i=1}^8 \mathbf{G}_i = \sum_{i=1}^8 \mathbf{F} N_i(x, y, z). \quad (14)$$

This is $\mathbf{G}_i = \mathbf{F} N_i(x, y, z)$. It can be shown that as the value of the shape functions $N_i(\mathbf{x})$ is proportional to the distance from the i -th node to the point of application of the force, the set of forces \mathbf{G}_i will preserve the total momentum of the original force \mathbf{F} .

with the advantage that shape functions are proportional to the distance from the i -th node to the point of application of the force.

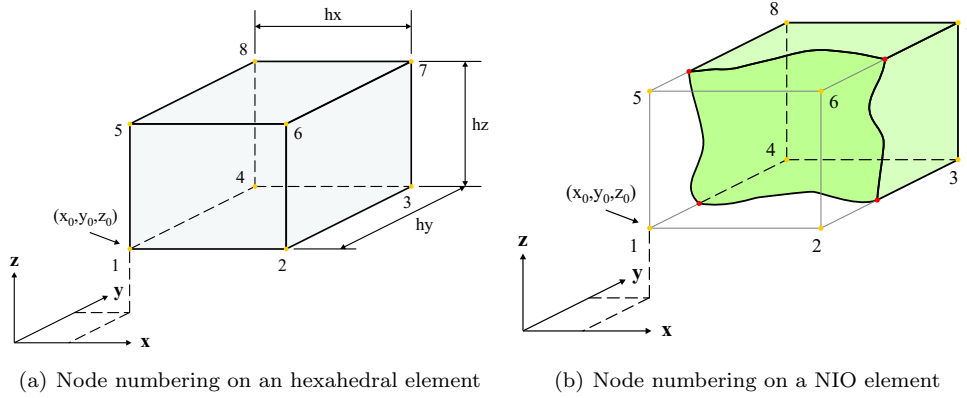


Fig. 5. Variables defining the hexahedral element

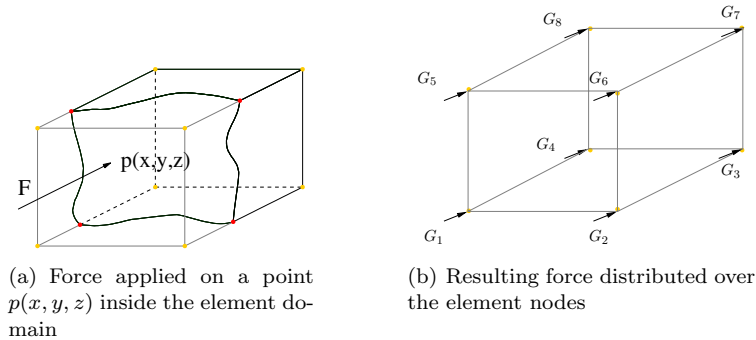


Fig. 6. A force applied on a point inside the domain can be approximated as a set of forces applied on the element nodes

5. Distributed forces

When distributed \mathbf{P} forces are applied over NIO element facets they also need to be translated into nodal forces. The total force over the element is given by $\int \mathbf{P} dA = \sum \mathbf{P}(\text{facet}) \times \text{Area}(\text{facet})$. This is, the force over a k -th facet inside an NIO element can be approximated as a force applied on the facet centroid. $\mathbf{F}^{(k)} = \mathbf{P}^{(k)} \times A^{(k)}$. Therefore the resulting force over an element can be obtained as a successive application of (14) over all the $\mathbf{F}^{(k)}$ forces.

6. Displacement boundary conditions

When a displacement boundary conditions is applied over an arbitrary point over the surface of the object it needs to be translated to the nodes of the FG.

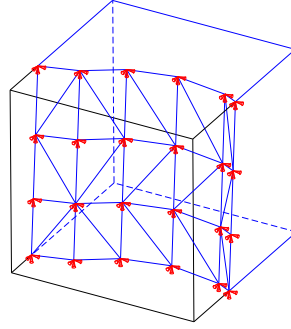


Fig. 7. NIO element with displacement restrictions on the model boundaries

Let again consider the shape element functions $N_k(x, y, z)$ over a finite element as in equation (12). If n_j represent any nodes at the element, then by definition of a base functions $N_k(n_j) = \delta_{kj}$, with δ_{kj} the Kronecker delta which is equal to one if $k = j$ and equal to zero otherwise. As it was shown in the last section, if a point \mathbf{x} is at the inside of a element, then the value of the shape functions $N_k(\mathbf{x})$ will be proportional to the proximity to the n_k node (e.g., if a point \mathbf{x} is at the center of an element, the element shape functions evaluated at this point are all equal to $\frac{1}{8}$). This feature can be used as a metric to calculate the proximity of a point to a node. By using this property from the element shape functions, the nodes which are closer to a point p inside the element domain, inherit the displacement boundary condition applied to the point p . This criteria can be applied selectively in the following way:

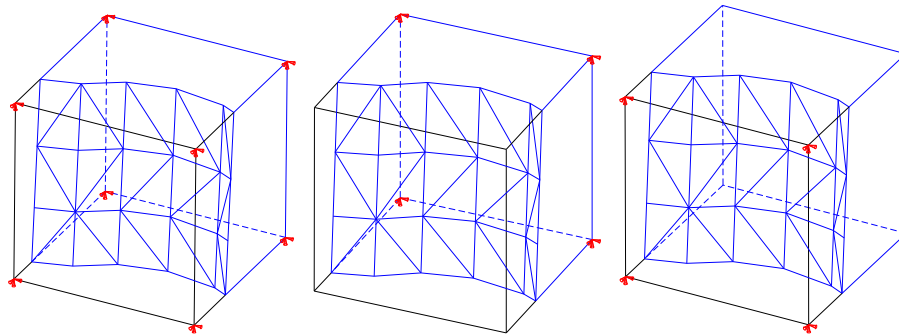
- (1) All the nodes in the *NIO* element inherit the displacement boundary condition [Figure 8(a)];
- (2) Only the *I* nodes inherit the displacement boundary condition [Figure 8(b)];
- (3) Only the *O* nodes inherit the displacement boundary condition [Figure 8(c)].

With the conditions enumerated above, a point equidistant to the nodes, can be included or excluded from the boundary condition translation in order to avoid all the nodes from inheriting the boundary condition applied to a central point.

7. Numerical test

These examples show the capabilities of the FG method. Due to the lack of analytical solutions the FG method is compared with solutions obtained using commercial finite element software. For simplicity in all cases, the properties of the material were chosen to be $E = 1 \times 10^9$ and $\nu = 0.2$.

In order to compare the Fixed Grid Finite Element Analysis (FG-FEA) against classical FEA a vector \mathbf{d} of displacements is defined as $d_i = \sqrt{u_1^2 + u_2^2 + u_3^2}$. That is d_i is the norm of the displacement \mathbf{u} at node i . The displacement error can be



(a) Displacement restrictions transferred to all the nodes of the NIO element (b) Displacement restrictions transferred to the inside nodes of the NIO element (c) Displacement restrictions transferred to the outside nodes of the NIO element

Fig. 8. Transference of the displacement boundary condition to the nodes of an NIO element.

defined as

$$E_r = \frac{\|\mathbf{d}_{FG} - \mathbf{d}_{real}\|_\infty}{\|\mathbf{d}_{real}\|_\infty}, \quad (15)$$

where \mathbf{d}_{real} corresponds to a theoretical result of the same experiment. This value can be obtained based on convergence analysis of the FEA solution and using a technique such as Richardson extrapolation [García (1999a)].

7.1. *L beam example*

This example consists of an L-shaped beam. It is fixed at one extreme and loaded with a shear force at the other end as shown in Figure 9. The maximum displacement was found to be located along the line formed by points (75, 0, 100) and (75, 25, 100). Applying Richardson extrapolation to the displacement found by FEA, a value of 5.84930×10^{-5} was obtained. This value was compared with the results obtained with different densities of grids. These are shown in Table 1.

Table 1. Displacement error and comparison with classical FEA for the example of the L-shaped beam

| Mesh size | dof | $\ \mathbf{d}\ _\infty$ FEA | % Error | $\ \mathbf{d}\ _\infty$ FG-FEA | % Error |
|-----------|------|--------------------------------|---------|-----------------------------------|---------|
| 3x1x4 | 108 | 6.322×10^{-6} | 89.2 | 6.037×10^{-6} | 89.7 |
| 6x2x8 | 540 | 1.866×10^{-5} | 68.1 | 1.766×10^{-5} | 69.8 |
| 12x4x16 | 3240 | 5.724×10^{-5} | 2.2 | 5.385×10^{-5} | 7.9 |

In this test, the only difference with classical FEA is the inclusion of O elements

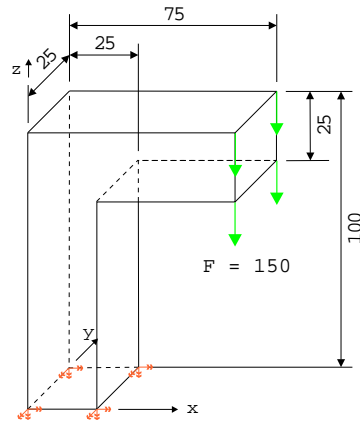


Fig. 9. Boundary conditions for the L-shaped beam problem

into the stiffness matrix. In spite of the fact that the material properties of the O elements are chosen to be those of non-active media, they can not be chosen as zero because this will result into singularities of the system matrix. As a consequence, inclusion of O elements will increase the stiffness of the overall structure. Nevertheless, it is observed that the error decreases as the density of the mesh does.

7.1.1. Exclusion of O elements

Due to the increased stiffness caused by the presence of the O elements the same test was accomplished without considering the O elements. As it was expected in this case, the result of the FG was equal to that obtained with classical FEA. However, when comparing the solution time of inclusion-exclusion of O elements, a reduction of 50% was obtain when O elements were excluded [Ruiz (2001)]. There are two factors that explain this time reduction: one is the reduction in the degrees of freedom of the system, and second, the reduction in the condition number of the stiffness matrix. The condition number is an indicator of how close to singularity a matrix is and has a consequence in the number of iterations used to find the solution when a preconditioned conjugate gradient method is used. The condition number for a system of equations $[K]u = f$ is defined by $\kappa(K) = \|K\|\|K^{-1}\|$. If $\kappa(K)$ is close to one, then the matrix is well conditioned. Otherwise, if $\kappa(K)$ is large then the matrix is ill-conditioned. This condition number was calculated for different stiffness matrices of the L beam example. The results are shown in Table 2. It is observed that there is a sharp increase of the condition number when including the O elements in the solution.

Table 2. Comparison of the condition number for the stiffness matrix when including and excluding the O elements.

| Mesh size | $\kappa_2(K)$ | |
|-----------|------------------------|------------------------|
| | Including O elements | Excluding O elements |
| 2x2x1 | 9240.1790 | 79.9036 |
| 4x4x2 | 25438.5042 | 406.5693 |
| 8x8x4 | 66744.1386 | 1469.0489 |
| 16x16x8 | 256789.2165 | 5325.2153 |

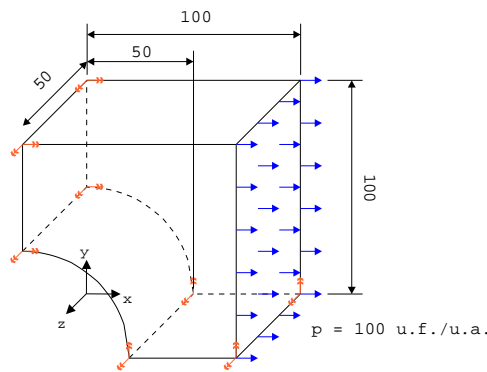


Fig. 10. Schematic view of a quarter of the square plate with a circular hole.

7.2. Square plate with a circular hole

This numerical experiment uses a square plate with a circular hole. Figure 10 shows the dimensions and boundary conditions of the structure. Due to the symmetry of the problem, only a quarter of the object is analysed.

The test was intended to observe the behaviour of the method when modelling a structure with NIO elements. The test also considers the inclusion of O elements into the construction of the stiffness matrix. Using an FEA solver, a maximum displacement of 3.835×10^{-5} was found along the line formed by points $(100, 0, 0)$ and $(100, 0, 50)$. (The FEA solver used a mesh of 6750 elements, 7936 nodes and 22784 degrees of freedom.) This calculated value was used to determine the displacement error of the FG method.

The results are presented in Table 3 for A0 approximation and in Table 4 for A1 approximation. Similar results were obtained in both cases. It is observed that the error has a marked oscillatory behaviour. However, it does decrease as the element size decreased.

Table 3. A0 approximation of NIO elements

| Mesh size | with O elements | | | without O elements | | |
|-----------|-----------------|-------------------------|--------|--------------------|-------------------------|-------|
| | dof | $\ \mathbf{d}\ _\infty$ | Error | dof | $\ \mathbf{d}\ _\infty$ | Error |
| 4x4x2 | 189 | 4.2199×10^{-5} | 9.18% | 180 | 3.7293×10^{-5} | 3.52% |
| 8x8x4 | 1115 | 4.4129×10^{-5} | 14.17% | 995 | 4.1426×10^{-5} | 7.18% |
| 10x10x5 | 2034 | 4.2931×10^{-5} | 11.07% | 1800 | 4.0555×10^{-5} | 4.92% |
| 16x16x8 | 7479 | 4.3226×10^{-5} | 11.83% | 6372 | 4.1093×10^{-5} | 6.31% |
| 20x20x10 | 14069 | 4.1854×10^{-5} | 8.28% | 11858 | 3.9840×10^{-5} | 3.07% |
| 32x32x16 | 54383 | 4.1684×10^{-5} | 7.84% | 45050 | 3.9812×10^{-5} | 3.00% |

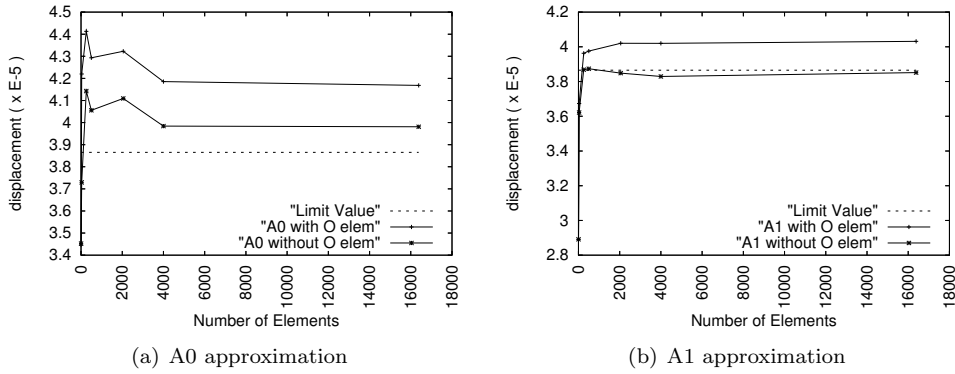


Fig. 11. Convergence plots for discrete (a) and weighted average (b) approximation of NIO elements

Table 4. A1 approximation of NIO elements

| Mesh size | with O elements | | | without O elements | | |
|-----------|-----------------|-------------------------|-------|--------------------|-------------------------|-------|
| | dof | $\ \mathbf{d}\ _\infty$ | Error | dof | $\ \mathbf{d}\ _\infty$ | Error |
| 4x4x2 | 189 | 3.6736×10^{-5} | 4.96% | 180 | 3.6215×10^{-5} | 6.31% |
| 8x8x4 | 1115 | 3.9627×10^{-5} | 2.52% | 995 | 3.8685×10^{-5} | 0.08% |
| 10x10x5 | 2034 | 3.9755×10^{-5} | 2.85% | 1800 | 3.8739×10^{-5} | 0.22% |
| 16x16x8 | 7479 | 4.0204×10^{-5} | 4.01% | 6372 | 3.8483×10^{-5} | 0.44% |
| 20x20x10 | 14069 | 4.0199×10^{-5} | 4.00% | 11858 | 3.8294×10^{-5} | 0.93% |
| 32x32x16 | 54383 | 4.0316×10^{-5} | 4.30% | 45050 | 3.8516×10^{-5} | 0.35% |

7.3. Re-analysis

The last numerical experiment deals with re-analysis using the FG method. Figure 12 shows the structure and boundary conditions used. The geometry of the

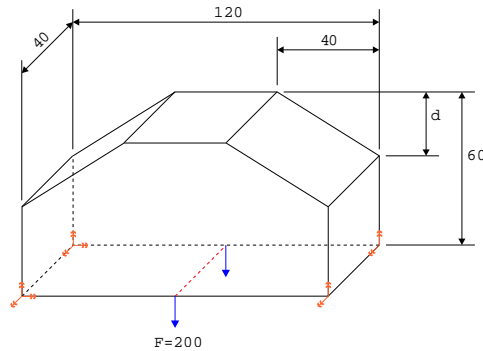


Fig. 12. Geometry and boundary conditions for structure used to test reanalysis capabilities of the FG method

object is expressed in terms of the parameter d . Variations to its dimension will result in different geometries. Initially a value of $d = 10$ was used. Then it was change to $d = 20$ and $d = 30$ respectively. In this case the Ω_{FG} is maintained constant and if O elements are kept the structure of the stiffness matrix is also maintained. The new stiffness matrix is given by $[K]^{new} = [K]^{old} + \Delta[K]$. $\Delta[K]$ is obtained by recomputing the element stiffness matrix of the elements whose I, O, NIO state changed as a result of the geometry variation.

The problem was solved for the initial case and then the stiffness matrix was modified to suit the structure with $d = 20$ and $d = 30$. The results are summarised in table 5. They are compared with the results obtained using commercial FEA software. The reanalysis procedure showed savings in time of 45% in the first case and 28% in the second case.

Table 5. Re-analysis test and comparison with FEA

| case | u_r-FEA | u_r-FG | Error | Time [s] |
|------|--------------------------|--------------------------|---------|----------|
| 0 | 2.02801×10^{-7} | 2.01282×10^{-7} | 0.7493% | 9.28519 |
| 1 | 2.08286×10^{-7} | 2.17141×10^{-7} | 4.2511% | 5.07962 |
| 2 | 2.17406×10^{-7} | 2.17094×10^{-7} | 0.1437% | 6.67140 |

8. Performance

In order to compare the performance of the FG method with classical FEA, the structure of example 7.2 was solve for different mesh sizes using commercial FEA software and FG. In each case the mesh was uniformly refined. For classical FEA,

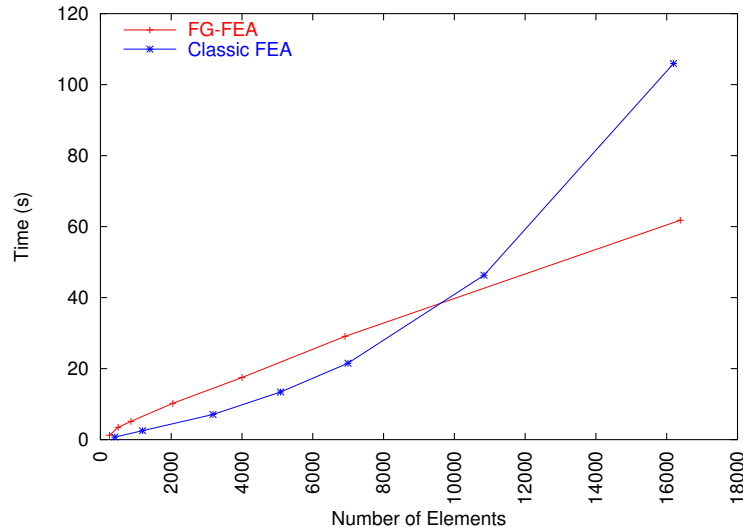


Fig. 13. Comparison of the FG and classical FEA computing times for the plate with circular hole structure.

ANSYS 8.0[©] was used. The element type was chosen as a 10 node tetrahedral element and the preprocessing used Delone triangulation. The solver used preconditioned conjugate gradient. In order to avoid the delay due to user interaction, the program was run in batch mode. The FG solver used an eight node cubic element, the elements O were excluded, and the solver used preconditioned conjugate gradient with Jacobi preconditioner. NIO reconstruction and volume calculation was accomplished using a qhull algorithm [Barber *et al.* (1996)] over the points generated by the intersection $e_m \cap \Omega$ for each e_m such that $\text{type}(e_m) = NIO$. The test was accomplished using a Pentium 4[©] 2.4 GHz with 512 RAM.

The results are presented in Figure 13. The total preprocessing plus solution time is plotted as a function of the number of nodes. It can be observed that classic FEA requires less time than FG for small number of elements. However, as the number of elements increases FG method perform faster than classical FEA revealing a smaller order of complexity that offers the FG-method. Also, it has to be considered than in an real situation the classical FEA will have to cover interaction time that was not included in this experiments.

9. Conclusions

This article presents a method for numerical analysis using a fixed grid three-dimensional domain. The program developed takes a structure previously constructed with a conventional solid modeller program and produces its fixed grid representation. Special care is taken when obtaining the intersection of the object with the grid in such a way that the elements preserve the geometry of the object.

The stiffness matrix of the system is obtained as a function of a unique element stiffness matrix thus saving time in its assembling.

The Boundary of the object is translated into *NIO* elements. The geometric shape of the elements is capture through NIO elements. Although it is an approximation of the actual shape reducing the accuracy of the results it also acts as an automatic defeaturing procedure that should be accomplished when porting structures from a geometric modeller. This feature helps reducing the transition CAD-analysis.

The displacement error obtained in the numerical test was found to be from 8 to 15 %. Therefore, the usefulness of method as a fast estimator of the displacement and stress fields is observed. However, good accuracy will require a large number of elements.

When analysing structures whose shape is similar to a shell or thin plate, the number of elements required to properly model the geometry is too large and makes impractical its applicability unless that *O* elements are excluded from the analysis.

Inclusion of *O* elements in the construction of the stiffness matrix increases the degrees of freedom of the system and produces ill-conditioned matrix. However, when keeping *O* elements the matrix structure remains constant under small changes in the geometry and therefore reduces the computational cost of reanalysis. Finally the performance of the method overtakes the classic finite element analysis performance as the number of elements increases.

Acknowledgements

The support by EAFIT-COLCIENCIAS under contract 572-2003 is gratefully acknowledged.

References

- Fagan, M. J. (1992). *Finite Element Analysis*, Longman.
- García, M. J. and Steven, G. P. (1999). Displacement error for fixed grid finite FEA elasticity problems. *III Congreso Colombiano en Elementos Finitos y Modelación Matemática*, Medellín, October 10-11.
- García, M. J. and Steven, G. P. (1997). Interactive aerospace design using fixed grid finite element analysis. *International Aerospace Congress, Sydney*, February.
- García, M. J. and Steven, G. P. (1998). Optimisation of Structures by Using Fixed Grid Representation of the Finite Element Domain. *Australasian Conference on Structural Optimisation*, Sydney, Australia, February.
- García M. J. (1999). Fixed Grid Finite Element Analysis in Structural Design and Optimisation. Ph.D. Thesis, Aeronautical Engineering, The University of Sydney, Sydney, Australia.
- García, M. J. and Steven, G. P. (1999). Fixed grid finite elements in elasticity problems. *Engineering Computations*, **16**, 2, pp. 145–164.
- García, M. J. and Steven, G. P. (2000). Fixed Grid Finite Element Analysis in Structural Design and Optimisation. *Second ISSMO/AIAA Internet Conference on Approximations and Fast Reanalysis in Engineering Optimization*, Delft, May 25-June 2.

- García, M. J. and Gonzalez, C. A. (2004). Shape Optimization of Continuum Structures Via Evolution Strategies and Fixed Grid Finite Element Analysis. *Journal of Structural and Multidisciplinary Optimization*, January, **26**, 1-2, pp. 92–98.
- García, M. J., Ruiz, O., Ruiz, L. M., Querin, O. (2004). Fixed Grid Finite Element Analysis for 3D Linear Elastic Structures. *VI World Congress on Computational Mechanics*, Beijing, China, Sept.
- Kim, H., García, M. J., Querin, O. M., Steven, G. P. and Xie, Y. M. (2000). Fixed Grid Finite Element Analysis in Evolutionary Structural Optimisation. *Engineering Computations*, **17**, 4, pp. 427–439.
- Kim, H., García, M. J., Querin, O. M., Steven, G. P., and Xie, Y. M. (2000). Fixed Grid Finite Element Analysis in Evolutionary Structural Optimisation. *Engineering Computations*, **17**, 4, pp. 427–439.
- Mobley, A. V., Carroll, M. P. and Canann, S. A. (1998). An Object Oriented Approach to Geometry Defeaturing for Finite Element Meshing. *7th International Meshing Roundtable, Sandia National Labs*, Dearborn, Michigan, U.S.A., October 26–28, pp. 547–563.
- Ruiz, L. M. (2001). Elementos Finitos de Malla Fija en tres Dimensiones. *Tesis Pregrado Universidad EAFIT*.
- Suzuki, K., Ohtsubo, H. and Terada, K. (1998). The Analysis of 3D Solid using Multi-Scale Voxel Data. *IV World Congress on Computational Mechanics*, Buenos Aires, Argentina, June.
- Woon, S. Y., Querin, O. M. and Steven, G. P. (2000). Application of the fixed-grid FEA method to step-wise GA shape optimisation. *Proceedings of second ASMO-UK /ISSMO conference*, Swansea, UK, pp. 265–272.
- Zienkiewicz, O. and Taylor, R. (1994). *El Metodo de los Elementos Finitos: Formulacion Basica y Problemas Lineales*, volume 1, 4th edn. Mc-Graw Hill.
- Barber, C. B., Dobkin, D. P. and Huhdanpaa, H. (1996). The quickhull algorithm for convex hulls. *ACM Trans. Math. Softw.* **22**, 4, pp. 469–483.